



Influence of viscous flow relaxation time on self-similarity in free-surface jet impingement



Wilko Rohlf s^{a,*}, Claas Ehrenpreis^a, Herman D. Haustein^b, Reinhold Kneer^a

^a Institute of Heat and Mass Transfer, RWTH Aachen University, Augustinerbach 6, 52056 Aachen, Germany

^b School of Mechanical Engineering, Faculty of Engineering, Tel Aviv University, Ramat Aviv, Tel Aviv 69978, Israel

ARTICLE INFO

Article history:

Received 20 January 2014

Received in revised form 30 June 2014

Accepted 30 June 2014

Available online 25 July 2014

Keywords:

Free-surface jet impingement

Local heat transfer

Convective heat transfer

ABSTRACT

Self-similar behavior in laminar free-surface jets regarding the velocity profile, its evolution, and the influence on stagnation-region heat transfer is presented. Approximate theoretical analysis shows that there are two regions with different scaling: a free-jet region where viscous relaxation dominates and an impingement region where a potential solution applies. Using the dimensionless time scale found for the first region, $H/(D \cdot Re)$, self-similarity is obtained for the axial velocity and its development. Fully resolved numerical simulations are performed to identify the crossover between the regions. It is further shown that the velocity profile at the cross-over point directly dictates the heat transfer distribution in the stagnation zone. The conditions under which this distribution has a central or off-center peak are found to be related to specific velocity profiles. Numerical results are used to find approximate closed-form relations tying the jet emergence velocity to the heat transfer distribution. A new comprehensive correlation is subsequently formulated for the heat transfer incorporating this new time scale, covering the range of velocity profiles emerging from pipe-type (parabolic) to orifice-type nozzles (uniform). A well-known analytical Prandtl dependency for stagnation flows is employed, yielding strong agreement with the numerical results. Agreement is observed for a very wide range of liquid and laminar flow conditions (i.e., $0.07 < Pr < 1307$, $73 < Re < 2000$, and $4 < H/D < 110$).

© 2014 Elsevier Ltd. All rights reserved.

1. Introduction

Impinging jets are well known for their high heat/mass transfer rates and are thus widely used in industrial cooling and drying processes. In recent years, laminar flow conditions became more important due to the development of micro-jet cooling systems. Further, oil jet piston cooling involves free-surface jets of low Reynolds number ($Re < 4000$) [1]. Heat transfer characteristics of jets have been the subject of many experimental, analytical and numerical studies, as presented in comprehensive reviews [2–4]. From an application point of view, the prediction of heat transfer characteristics is of great importance to the design of specific processes. Traditionally, this is done by employing well-known empirical correlations developed from the data of several specific studies and typically found in handbooks on heat transfer. However, to gain a more scientific understanding and to develop physically based correlations, a fundamental approach is required, therein identifying inherent self-similarities. Once the basic underlying mechanisms have been understood, the most relevant

dimensionless parameters can be used to develop a more general model, whose weighting coefficients can be found using a wide range of experimental and numerical data.

Traditionally, the problem of heat transfer under jet impingement conditions is described by three dimensionless parameters: the Reynolds number, $Re = uD/\nu$, the Prandtl number, $Pr = \nu/\alpha$, and the nozzle-to-plate distance, H/D (where ν , α , u , and D denote the viscosity, thermal diffusivity, average velocity, and nozzle diameter, respectively). In dimensionless terms, the heat transfer is typically described by a correlation of the form

$$Nu = \frac{h \cdot D}{\lambda} = C \cdot Pr^\alpha Re^\beta \left(\frac{H}{D}\right)^\gamma \quad (1)$$

for both free-surface and submerged jets, where λ and h denote the thermal conductivity and convective heat transfer coefficient, respectively. The constants in the correlation, C , α , β , and γ , are found using experimental data and vary in the literature. The Prandtl number dependence of $\alpha = 1/3$ for liquids ($Pr > 10$) has been proposed on the basis of analytical [5] and experimental [6] observations. Values of $\alpha = 0.4$ and $\alpha = 0.37$ have been proposed for low ($Pr < 3$) and intermediate ($3 < Pr < 10$) Prandtl numbers, respectively. Regarding the Reynolds number dependency, values in the

* Corresponding author.

E-mail address: rohlfsw@wsa.rwth-aachen.de (W. Rohlf s).

range of $0.4 < \beta < 0.873$ have been found in experimental investigations [7,8], whereby lower values are usually associated with laminar flows and higher values with turbulent flows. However, analytical solutions [5,8] and the majority of experimental studies suggest a dependency around $\beta = 0.5$, a scaling well known from laminar boundary layer theory [9]. The nozzle-to-plate distance H/D strongly affects submerged impinging jets, where the surrounding liquid decelerates the jet rapidly through strong shear forces. For free-surface jets, correlations reported in several studies [8,10] suggest a weak dependency on H/D with an exponent ranging from $\gamma = -0.0336$ to $\gamma = -0.105$.

The relatively large variation of coefficients among different studies implies that additional physical aspects, such as the inlet velocity profile (affected by the nozzle type), jet inclination, temperature-dependent fluid properties (e.g., viscosity), and impingement surface geometry, are relevant to the impinging jet heat transfer problem. Some of these aspects have already been incorporated in previous studies, leading to aspect-specific correlations; e.g., correlations for specific nozzle types.

The present study takes a more fundamental approach whereby fully resolved numerical simulations are conducted to identify a new significant dimensionless scale leading to a more general form of Eq. (1). Therein, it is clearly shown that the heat transfer distribution in the impingement zone is directly related to the velocity profile of the incoming jet near the wall. In the case of free-surface jets examined here, this velocity profile is a result of the velocity profile of the jet emerging from the nozzle and of the process of viscous relaxation during the flight of the jet towards the wall. The conditions under which there is an off-center peak in the heat transfer distribution are identified, which has been previously been done only for *submerged jets* [11].

Considering the underlying hydrodynamic mechanisms, this study presents an explicit correlation for laminar jet impingement, which incorporates the new dimensionless time scale and is valid for a wide range of conditions and fluids (as defined by Re , Pr , and H/D).

Finally, the hydrodynamics and heat transfer in the wall jet region are investigated, revealing the transition between two different scaling behaviors. Good agreement between the analytical solutions of Watson [12] and Liu and Lienhard [13] is shown and suggestions for improving the analytically derived heat transfer correlations are given.

2. Numerical methods and boundary conditions

Numerical simulations of the axisymmetric free surface jet configuration are performed by solving the fully incompressible two-phase Navier–Stokes equations for mass

$$\frac{\partial \rho}{\partial t} + \frac{\partial \rho u_i}{\partial x_i} = 0 \quad (2)$$

and momentum

$$\frac{\partial \rho u_i}{\partial t} + u_j \frac{\partial \rho u_i}{\partial x_j} = -\frac{\partial p}{\partial x_i} + \eta \frac{\partial^2 \rho u_i}{\partial x_j \partial x_j}, \quad (3)$$

while employing the volume of fluid (VOF) method (see [14]) using the Open Field Operation and Manipulation library (OpenFOAM, see [15]). Note that axisymmetry of the problem is solved in a two-dimensional domain, which is specified as a wedge with an angle of 1 degree.

In the VOF approach, a scalar transport equation for the volume fraction α in the form

$$\frac{\partial \alpha}{\partial t} + \frac{\partial (u_i \alpha)}{\partial x_i} = 0 \quad (4)$$

is introduced together with an interface compression scheme (see also [15]) of the form

$$\frac{\partial \alpha}{\partial t} + \frac{\partial u_i \alpha}{\partial x_i} + \frac{\partial u_{i,r} \alpha (1 - \alpha)}{\partial x_i} = 0, \quad (5)$$

where $u_{r,i}$ is an artificial “compression velocity” that is used to counteract interface smearing by numerical diffusion. The surface tension force, f_i^σ , is calculated using the continuum surface tension model [16]:

$$f_i^\sigma = \sigma \kappa = -\sigma \bar{n} (\bar{\nabla} \cdot \bar{n}). \quad (6)$$

The surface curvature κ is determined by the second derivative of the volume fraction field α , which yields

$$\kappa = \frac{\bar{\nabla} \cdot \bar{\nabla} \alpha}{|\bar{\nabla} \alpha|} (\bar{\nabla} \cdot \bar{\nabla} \alpha). \quad (7)$$

The fluid properties are obtained through volume averaging of the respective phase properties:

$$\rho = \alpha \rho_1 + (1 - \alpha) \rho_2, \quad \mu = \alpha \mu_1 + (1 - \alpha) \mu_2. \quad (8)$$

For the temperature distribution, a scalar transport equation is solved, without back coupling between the temperature and the velocity or pressure (e.g., through buoyancy forces or temperature-dependent thermophysical properties). It is important to emphasize that dissipative heat generation is not accounted for in the numerical simulations. Thus, the Nusselt number estimated from the wall temperature is equivalent to the Nusselt number calculated from the adiabatic wall temperature in experiments.

The central-difference scheme is used for all spatial discretization and a first-order, bounded implicit scheme is applied for temporal discretization. The computational domain (see Fig. 1) consists of two parallel walls: a lower heated wall on which the jet impinges and an upper wall through which the jet emerges. At the boundaries of the two walls, a no-slip condition is imposed for the velocity, and at the radial border of the domain ($r/D > 10$), a boundary condition that allows for inflows and outflows is imposed. For the velocity inlet of the laminar jet, a constant parabolic profile in the radial direction is imposed.

The domain shown in Fig. 2 is spatially discretized by hexahedral cells with a cell size in the radial direction of $9 \cdot 10^{-4} D \leq \Delta r \leq 0.1 D$. The cell size in the axial direction near the wall corresponds to one-tenth of the characteristic viscous length scale (which is the maximum value of $y^+ = 0.16$ for the highest

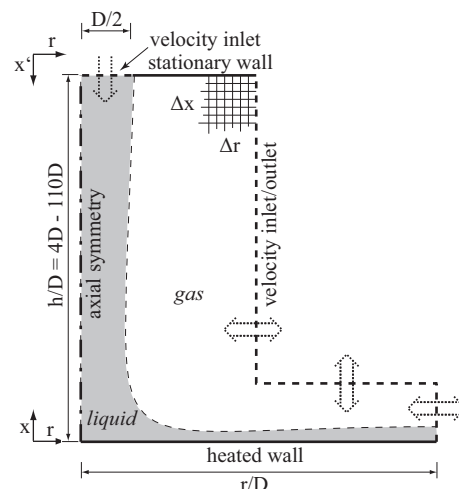


Fig. 1. Computational domain.

Download English Version:

<https://daneshyari.com/en/article/657712>

Download Persian Version:

<https://daneshyari.com/article/657712>

[Daneshyari.com](https://daneshyari.com)